CHAPTER 6

...and its dependence on some intrinsic properties of Mira Variables

6.1 Determination of Effective Temperature

The spectral-type of a Mira varies during its pulsation. The spectral-types listed in column 6 of Table 4.1, are from the General Catalogue of Variable Stars (Kholopov, 1985), in which they were compiled from several publications, and represent the extreme values during the pulsation cycle. It should be kept in mind that the sequence of spectral-types ranging from M0 to M10 represents an increase in the strength of the TiO absorption bands and a decrease in the photospheric temperature. The spectral-types for several Mira variables were measured by Keenan et al. (1974), at optical maximum, and by Lockwood and Wing (1972), throughout the pulsation period. Observationally, a large number of stars have been classified according to the spectral-types but a more physical quantity is the temperature. The calibration of the spectral-type with the represented effective temperature of the Mira variable, is still a subject full of uncertainties (Bessell et al. 1989).

The effective temperature is defined by the relation,

$$L = 4\pi R^2 \sigma T_{eff}^4, \qquad (1)$$

where L is the luminosity integrated over all frequencies, R is the radius of the star, σ is the Stefan-Boltzmann constant and T_{eff} is the effective temperature, assuming that the star emits like a black-body. In terms of observable quantities, one can express the effective temperature as (Whitelock 1986),

$$T_{eff} = 2341 (f_{bol})^{1/4} (\theta)^{-1/2}, \qquad (2)$$

where f_{bol} is the bolometric flux in 10^{-8} ergs cm^{-2} s^{-1}. and 8 is in milliarcseconds.

The earliest systematic measurements of effective temperatures and diameters of mira variables, assuming that they are black-body emitters, were made by Pettit and Nicholson (1933) They used a thermocouple at the focus of the 100" optical telescope* and measured a rise in the temperature of the order of 10^{-5} degrees centigrade over the background, as the star's image was made incident on the thermocouple. Since most of the energy is radiated in the infra-red, this measurement is approximately that of the bolometric magnitude. In addition, they obtained the effective temperature by measuring the change in the magnitude on introducing a water-cell (1 cm^3 of distilled water) in the optical path before the thermocouple. On doing an absorption experiment in the lab, they found that beyond about 1.5μ, most of the radiation is absorbed by water. If the incident radiation is that from a black-body, the ratio of the incident flux to the flux transmitted through the water-cell, is a function of temperature alone (calibrated experimentally). Thus one can measure the effective temperature of the source. Using this method they obtained the effective temperature of several Mira variables over different cycles of pulsation. Along with the measured bolometric magnitudes, they also obtained angular diameters of these Mira variables.

The effective temperature of Mira variables is a difficult quantity to measure reliably because the photosphere of a Mira variable itself is not well defined. Conventionally, one defines the radius of the photosphere as that distance from the center of the star at which the optical depth equals a value close to unity. Labeyrie et al. (1977) and Bonneau et al. (1982), have measured the angular diameters of some miras using speckle interferometry. They find that the diameter is a sensitive function of the wavelength, reaching differences of a factor of **3,**

*The Mt. Wilson Observatory

over wavelengths in the blue and visual range. The mean value of the diameter however, is in reasonable agreement with the ones obtained by indirect methods much earlier (Pettit and Nicholson, 1933). Robertson and Feast (1981) have found that for Mira variables, the colour temperature (obtained by fitting the black-body curve of that temperature to the observed fluxes at different wavelength) is in agreement with effective temperatures determined using diameters obtained from lunar occultation, at least for stars with periods ranging from 200 to 400 days. Bessell et al. (1989), on the other hand, find a discrepancy between these two temperatures, for two objects, S Vir and Z Sgr. Moreover, their model predicts the photospheric emission from Mira variables to be different from the black-body, and therefore, a systematic difference between the colour temperature and effective temperature.

Dyck et al. (1975) have obtained colour temperatures from black-body fits to their measured fluxes at 1.04 μ and 2.5 μ and have calibrated these colour temepratures with the effective temperatures of seven cool stars whose angular diameters have been measured. Their sample of stars contain Mira variables and IRC stars. The effective temperatures determined by this method, are listed in Table 1, and shown in Fig. 1, which also shows a fitted polynomial. This is the relation we have used in our study. One must note that the measured points are accurate to about half a division in spectral-type. Since most of the energy is emitted at infra-red wavelengths, it seems reasonable to adopt these temperatures which are obtained by measurements of fluxes and diameters at these wavelengths.

Table 1

Spectral-Type	Effective
M—	Temperature (K)
0	**3670**
1	**3600**
2	**3540**
3	**3460**
4	**3350**
5	**3220**
6	**3030**
7	**2790**
8	**2480**
9	**2090**
10	**1610**

6.2 The H–R Diagram for Mira variables

The absolute bolometric magnitudes from the P–L relation (eqn. 4 of Chapter 5), arid the effective temperatures obtained from spectral-types as mentioned in the earlier paragraph, are used to plot an H–R diagram for the Mira variables in our sample. This is shown in Fig. **2.** This figure may be compared with the H–R diagrams for Mira variables obtained previously by Scalo (1976), Tsuji **(1981)** and Wood et al. **(1983).** The H–R diagram given by these authors are mainly for M-giant stars, including very few Mira variables. As far as we know, Fig. 2 shows for the first time the evolutionary status of the masing and non-masing Mira variables. In Fig. **2,** the masing Mira variables are indicated by a cross and the non-masing ones by an 'o'. The two '#' symbols indicate the sources S Per and AH Sco, both of which are super-giants. Apart from these two sources, we note from Fig. **2** that the masing sources are restricted in the region $M_{bol} \leq -4.8$ magnitudes and $Log(T_{eff}) \leq 3.48$. This may be indicating the fact that a Mira variable has to attain a certain age before which the maser emission does not

occur. On the other hand, these limits on the bolometric magnitude and the effective temperature may be interpreted as a limit on the radius of the Mira variable above which it may show maser emission. We have,

$$M_{bol} = 42.31 - 5\log(\frac{R}{R_\odot}) - 10\log T_{eff}. \quad (3)$$

In this formula, using the limiting values of M_{bol} and log T found from Fig. 2, we get the result that the radius of the masing Mira variable should be $\geq 290 R_\odot$. A large value of radius may simply allow a larger path length for the gain of the maser, and hence a greater maser luminosity. Further, for a larger star, the density of gas in the envelope is expected to be lower, which is favourable for non-LTE conditions.

6.3 Correlation of maser luminosity with spectral-type and bolometric magnitude

In Figs. 3, we have plotted the maser flux, and the photon luminosity as a function of distance. These figures show that the maser sources are not equally luminous, and the variation in the luminosity is intrinsic to the source. Fig. 4 show the SiO maser photon-luminosity as a function of the mean spectral-type. The symbol '#' represents super-giants, whose intrinsic properties are expected to be different from that of the regular M-giant Mira variables. But for the two super-giants, all the masing Mira variables have spectral-types greater than M6. As the Mira variables approach the maximum brightness during their pulsation, their spectral class approaches an earlier type, corresponding to higher temperature. The value of spectral-type at the visual maximum epoch, below which there are no masing Miras, is therefore expected to be earlier than the limiting value of mean spectral-types. As seen in Fig. 5 this limiting spectral-type may

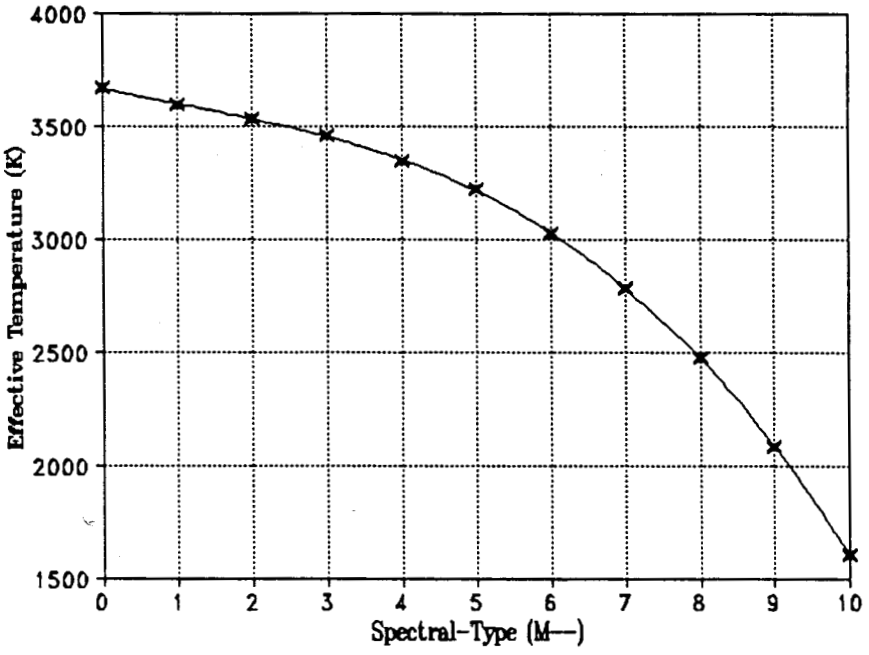

Figure 1: Obtaining effective temperatures from spectral-types. (Dyck et al. 1975)

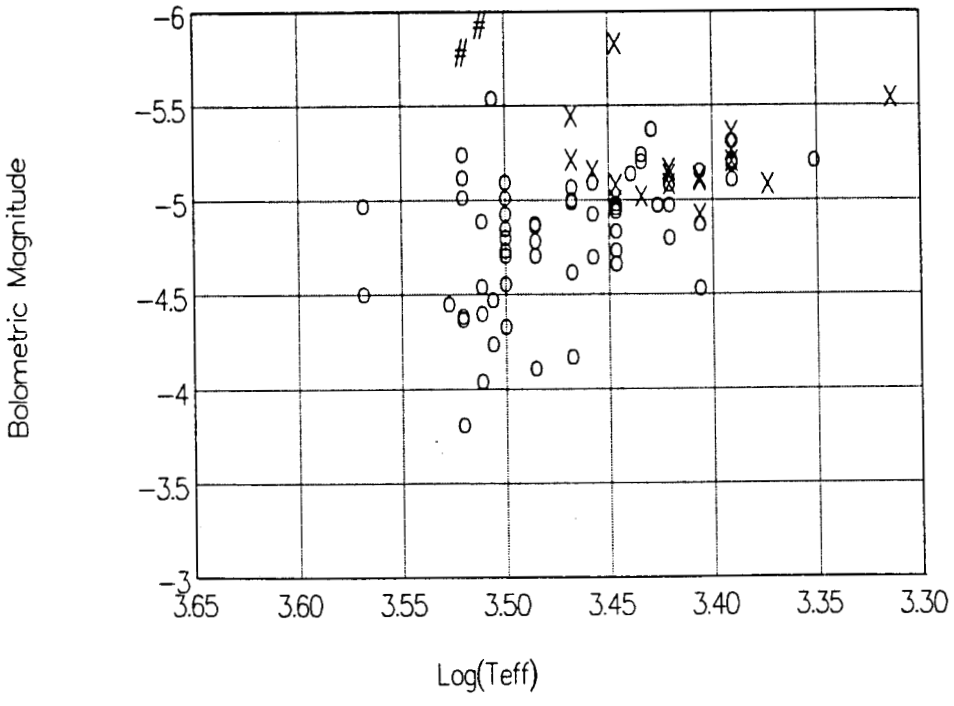

Figure 2: H—R diagram for the masing and non-masing Mira variables

reach M5, at its maximum phase during pulsation. Some of the sources for which we could find both the distance as well as the phase of pulsation at the time of observation are plotted in Fig. 6. Although this plot has a much smaller number of sources, we see that the masing Miras do not show a preferred value of spectral-type. Figs 7,8 & 9 are plots against effective temperatures instead of spectral-types. Corresponding to Fig. 6, in Fig. 9, where the spectral-type is converted to temperature, there does not seem to be any dependence of the maser luminosity on the effective temperature, once the Mira variable is in the masing range of temperatures, i.e., less than about 3100 K (see Fig. 7). In all these figures we notice that there are a substantial number of non-masers even in the range of spectral-types M6—M10. On the basis of time-variation of the maser luminosity (see Figs. 7.6), it may be that these sources were at phases which correspond to minimum SiO luminosity. To check this, we have made a histogram of phases for these objects which are non-detections in the mean spectral-type range M6—M10 (see Fig. 10). Although the number of sources in this histogram is rather small, there is no indication of a preferred phase in the number of non-detections. These sources are listed in Table 2. The other possible reasons for these non-detections are discussed in Chapter 7.

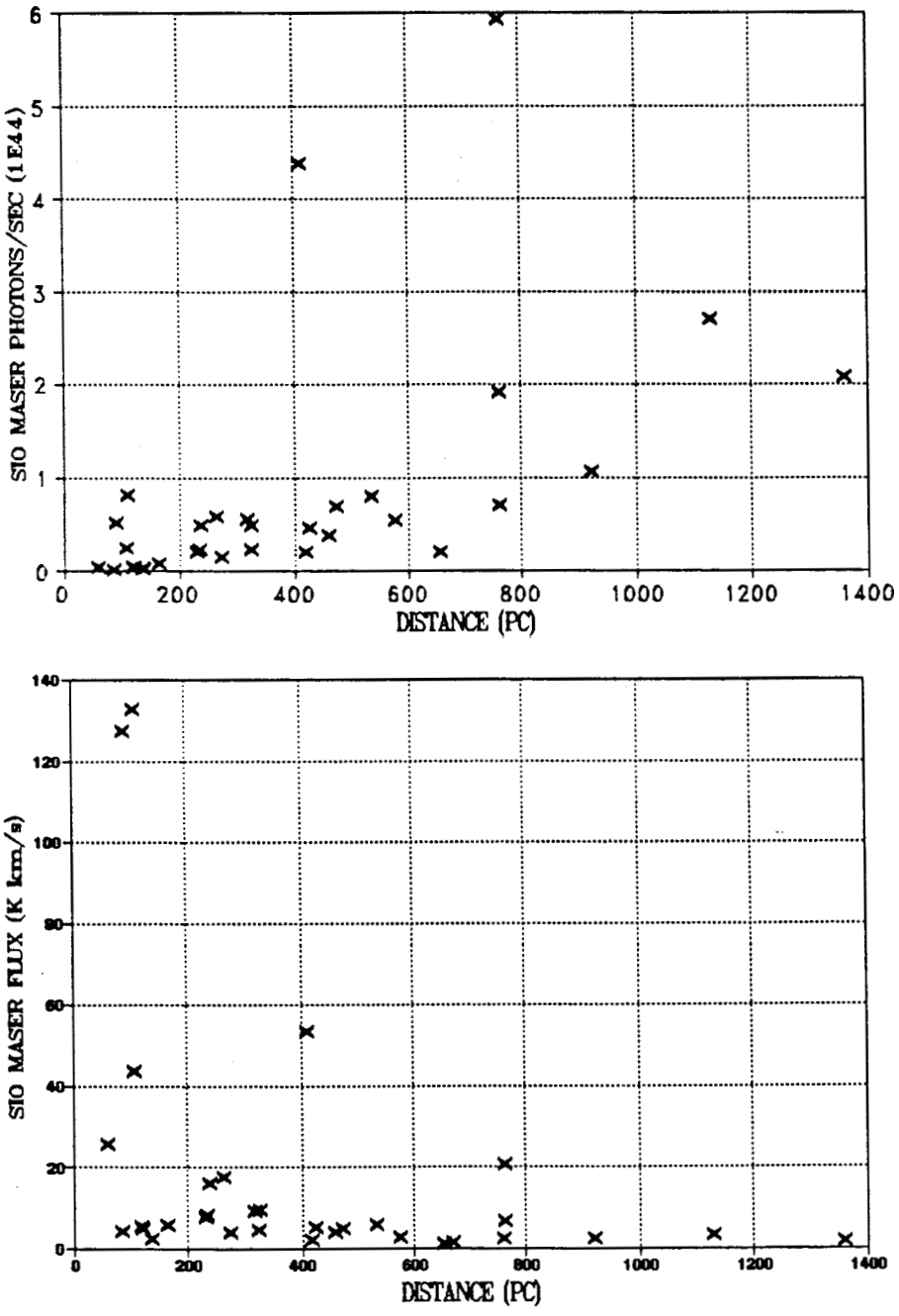

Figure 3: SiO maser flux and luminosity as a function of distance. These figures show that luminosity differs in different sources

Table 2: Non-detections later than M6

Source	Phase	Sp.Type
Ari U	0.74	6.75
Aur U	0.84	8
Cas Y	0.68	7.25
Cen RT	0.4	6.75
Cen V744	0.91	8
Cep T	0.85	7.15
Cnc W	0.33	7.75
Com R	0.23	6.5
Crt S		6.5
Crv R	0.95	6.75
Cyg Z	0.15	7
Eri W	0.39	8
Her RU	0.52	7.35
Hya RT		7
Lib FS	0.41	8.55
Lup R	0.26	6.75
Lyr RW	0.67	7
Ori DT	0.71	10
Ori S	0.92	8
Ser WX	0.64	8
Tau R	0.21	7
Vir BK	0.48	7

We see thus, that spectral-type later than M6 is a necessary but not a sufficient condition for masing.

Fig. 11 shows that the masing and non-masing sources separate out as a function of the bolometric magnitude. Thus, one more important criterion for maser emission seems to be the bolometric magnitude. In fact, many of the non-masers in the spectral-type range M6—M10 have bolometric magnitudes fainter than -4.8 magnitudes. This separation was also seen earlier in Fig. 2, the H–R diagram for Mira variables, where the maser luminosity was not indicated. Fig. 11 also indicates a correlation between the maser luminosity and the bolometric magnitude. We discuss this further in Chapter 7.

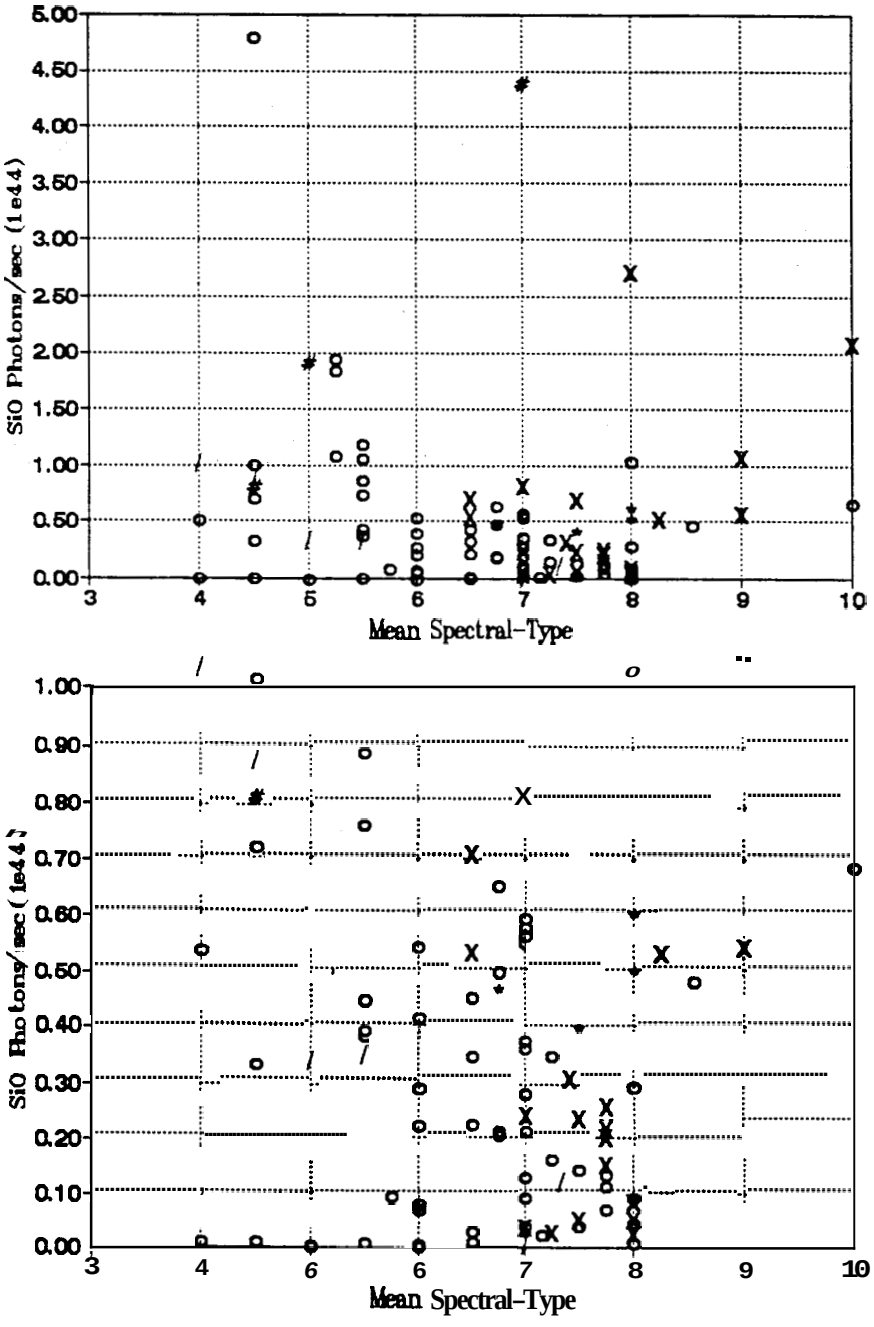

Figure **4:** Relation between the SiO maser-luminosity and the mean spectral-type. 'o' indicates upper limits,'x': detected sources and '#': supergiants. '/': non-detections at minimum phase (0.5—0.6), '*': detections at minimum phase

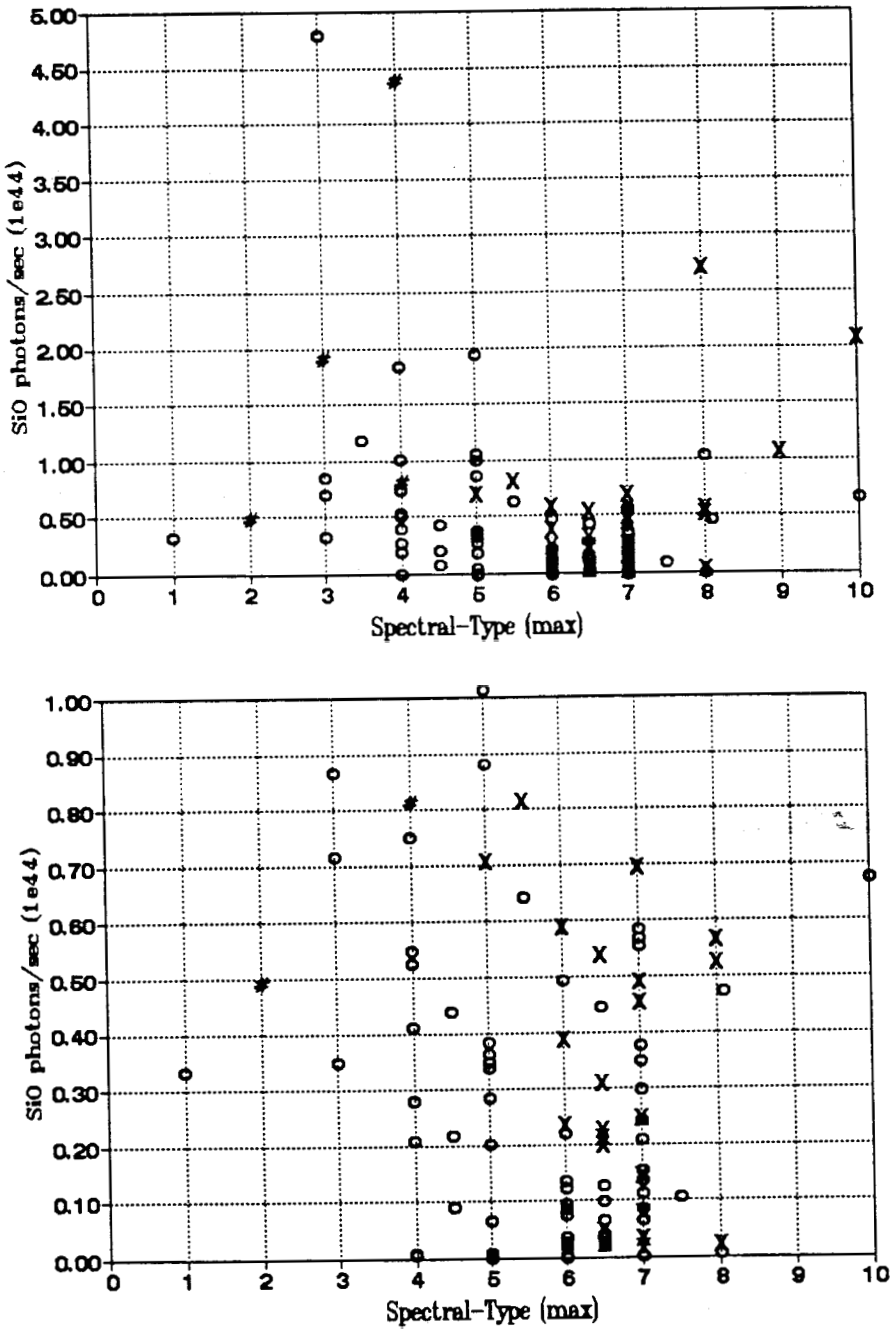

Figure 5: Same as Fig. 4 but for spectral-type at maximum light

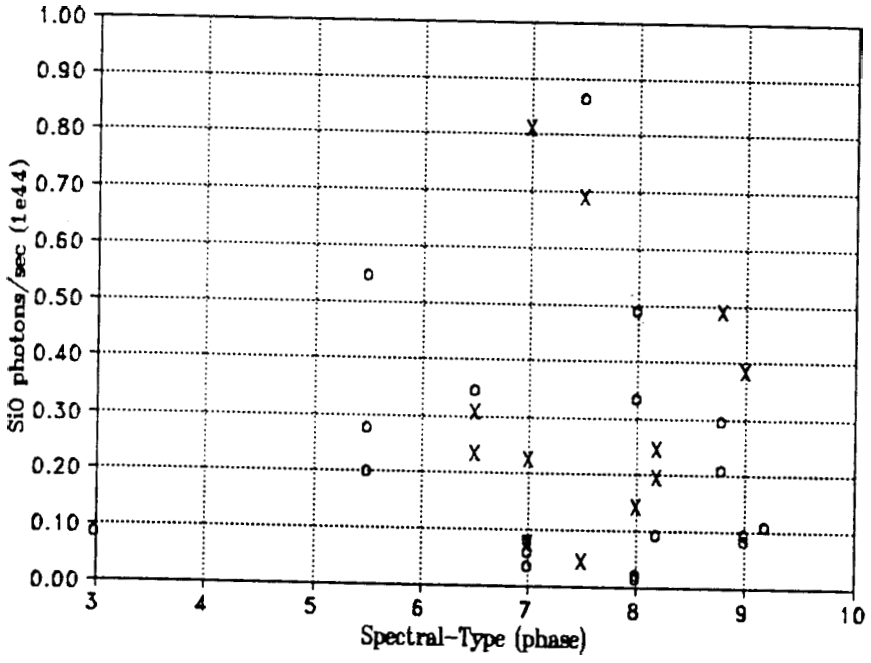

Figure 6: Same as Fig. 4 but for spectral-type at the pulsational phase on the date of observation

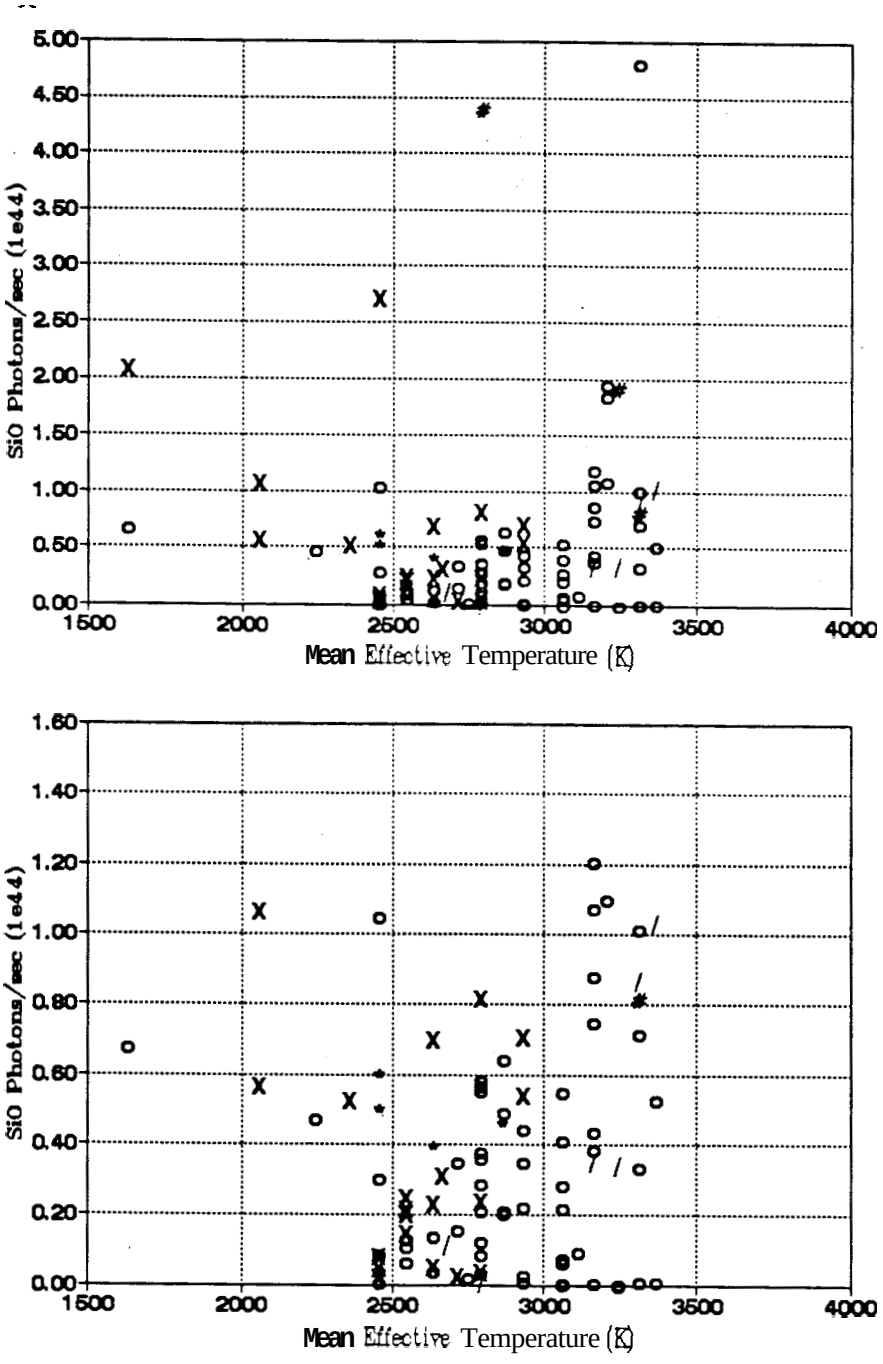

Figure 7: Same as Fig. **4,** with spectral-type converted to effective temperature

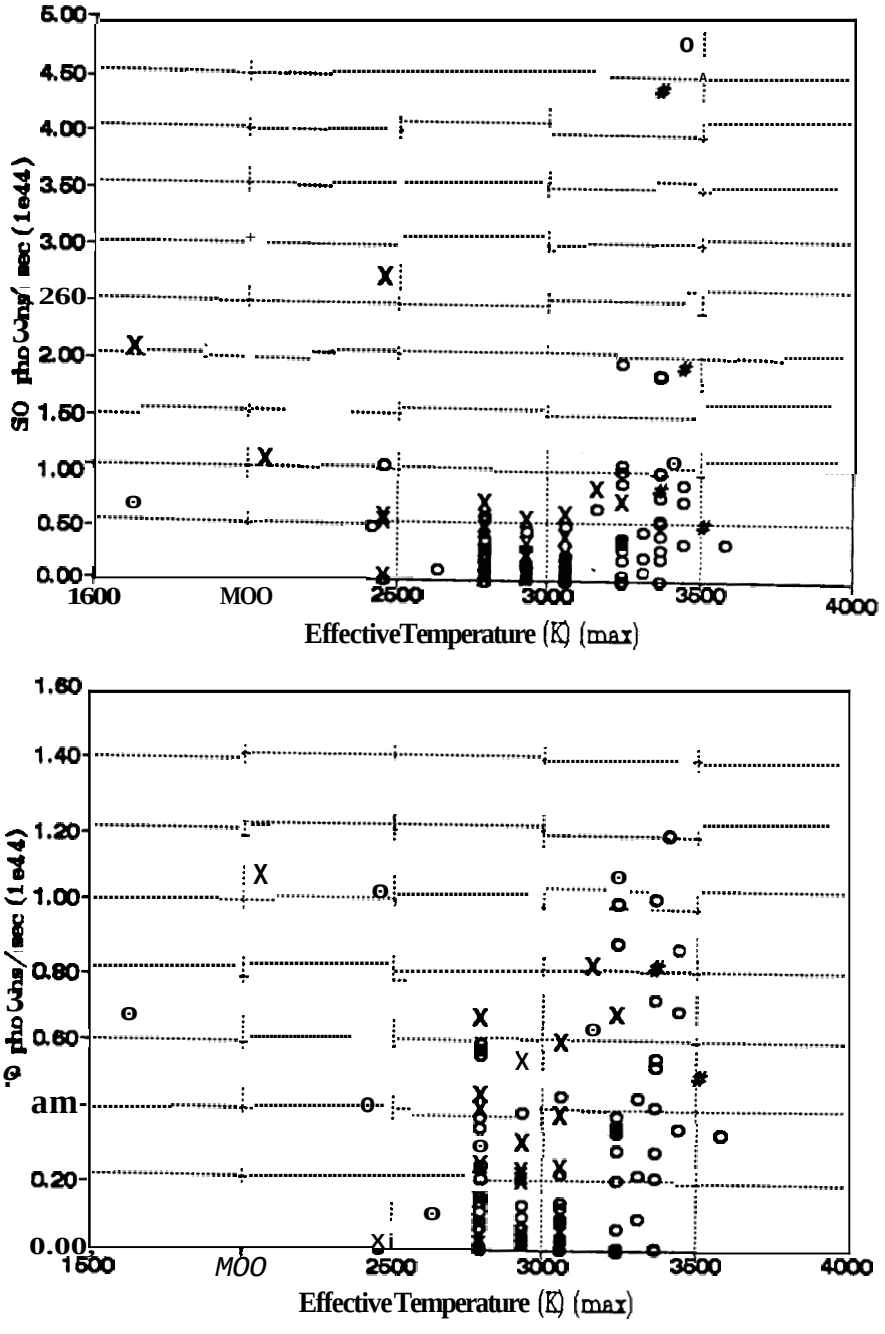

Figure 8: Same as Fig. 5, with spectral-type converted to effective temperature

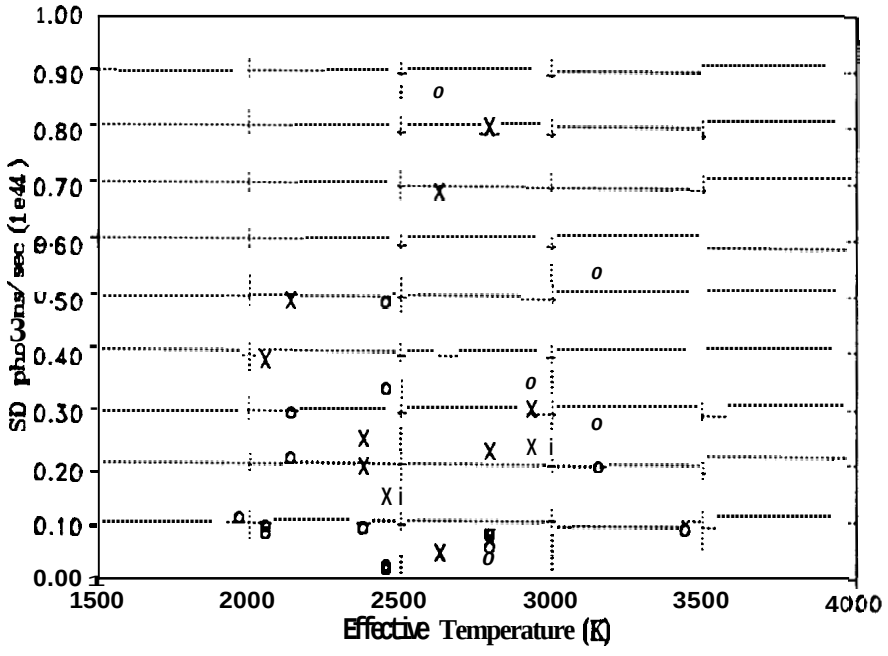

Figure 9: Same as Fig. 6, with spectral-type converted to effective temperature

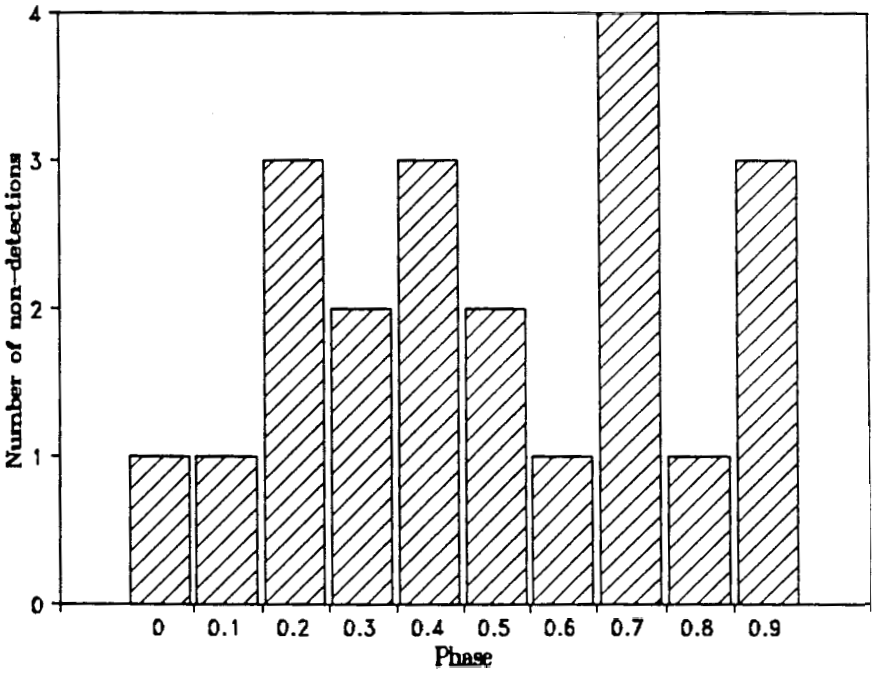

Figure 10: Histogram of pulsational phases of the non-detections

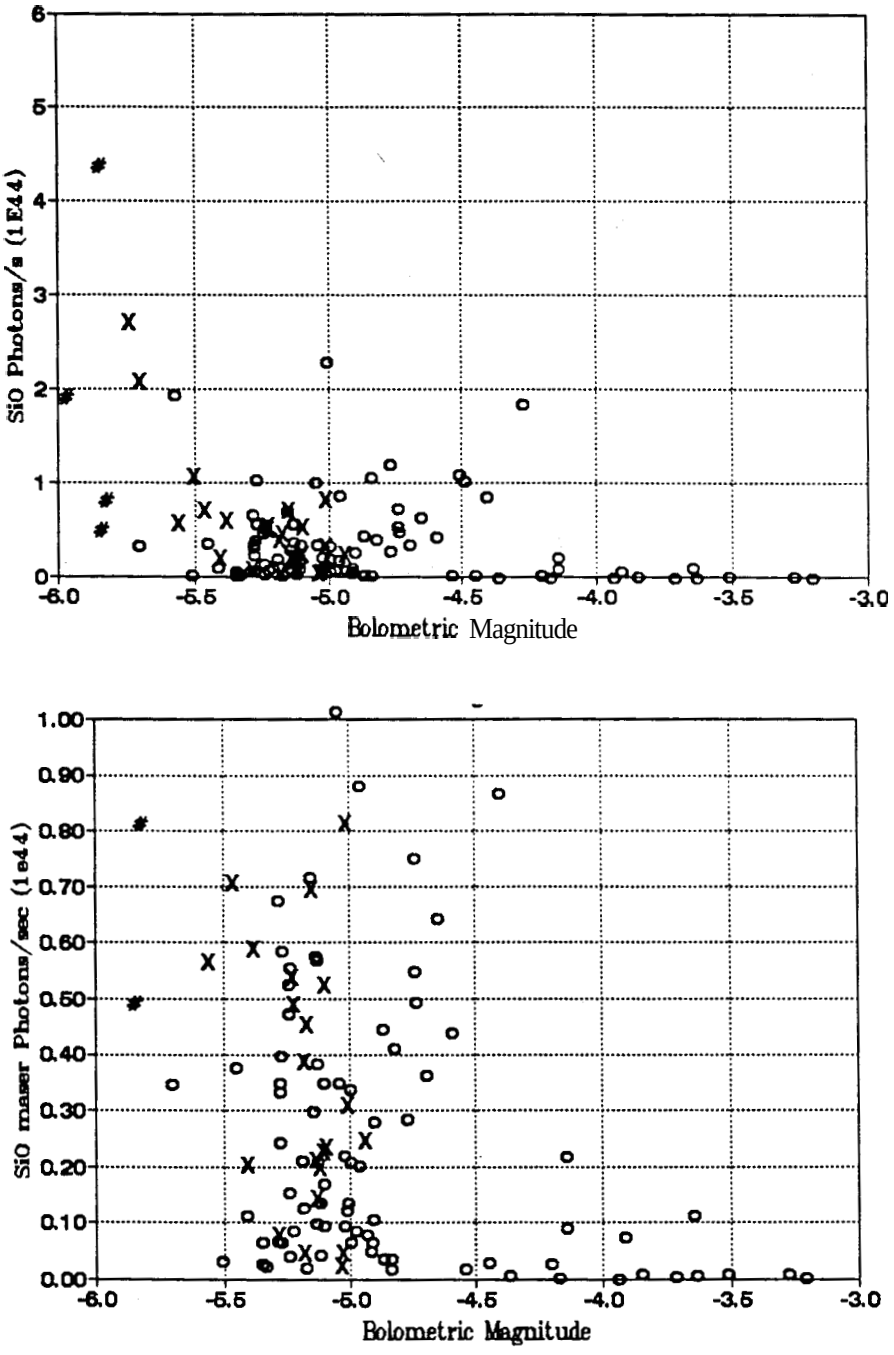

Figure 11: Correlation of maser luminosity with the bolometric magnitude

6.4 Correlation of maser luminosity with amplitude

Apart from the spectral-type and the bolometric magnitude, another possible intrinsic property of Mira variables to which the SiO maser may be related, is the visual amplitude of pulsation. It is well known that Mira variables show very large changes in the visual magnitude. The amplitude at infra-red wavelengths on the other hand. is much smaller (about 1 magnitude at infra-red, for an amplitude of about 5 magnitudes at visual). This is expected from the Planck function for two values of temperatures, which may be taken as 2000 K to 2500 K for a typical Mira variable. In addition there may be a temperature dependent opacity only at visual wavelength (Whitelock, 1990), which may increase the amplitude of pulsation at the optical wavelengths. Apart from changes in temperaturc, thc amplitude of pulsation will reflect changes in the diameter of the star; and since the SiO maser exists very close to the photosphere, one expects a physical connection between the maser process and the pulsational amplitude. To investigate this relation, we have plotted the SiO maser photon luminosity versus the pulsational visual amplitude in Fig. 12. There are four objects (two of them, super-giants) which have pulsational amplitudes less than 4 magnitudes and maser luminosities at least twice the values which the higher amplitude stars show. In Fig. 13, we have attempted to avoid the errors in the distances by plotting the ratio of the SiO maser flux to the SiO thermal (v=0) flux. The observed fluxes are also converted to their expected value at the maximum phase of pulsation, for the sources whose SiO light-curves are available.

The number of sources is very small because of lack of enough observations of the thermal SiO line. The thermal line observations used to obtain Fig. 13,

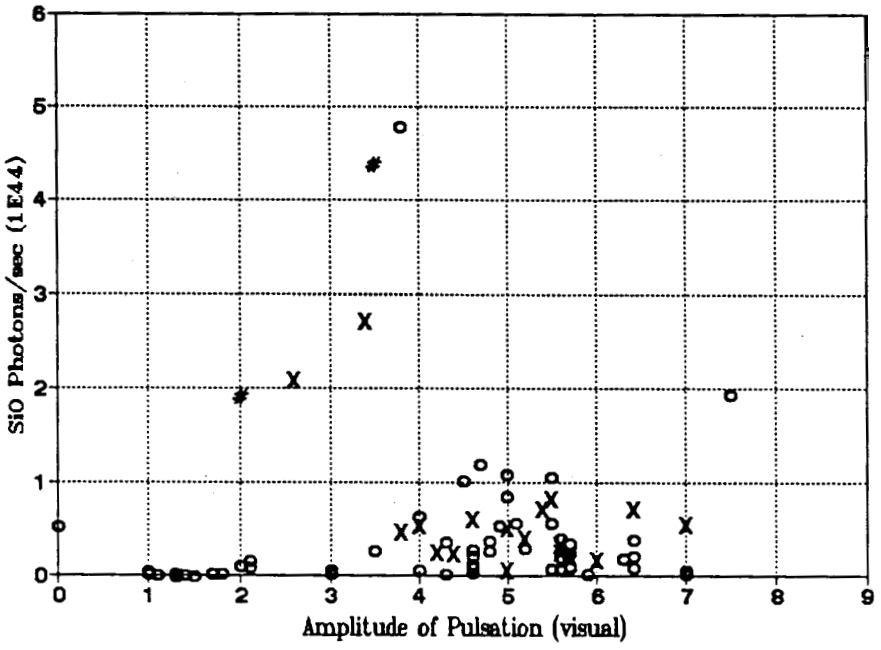

Figure 12: Relation between the maser luminosity and the visual amplitude of pulsation

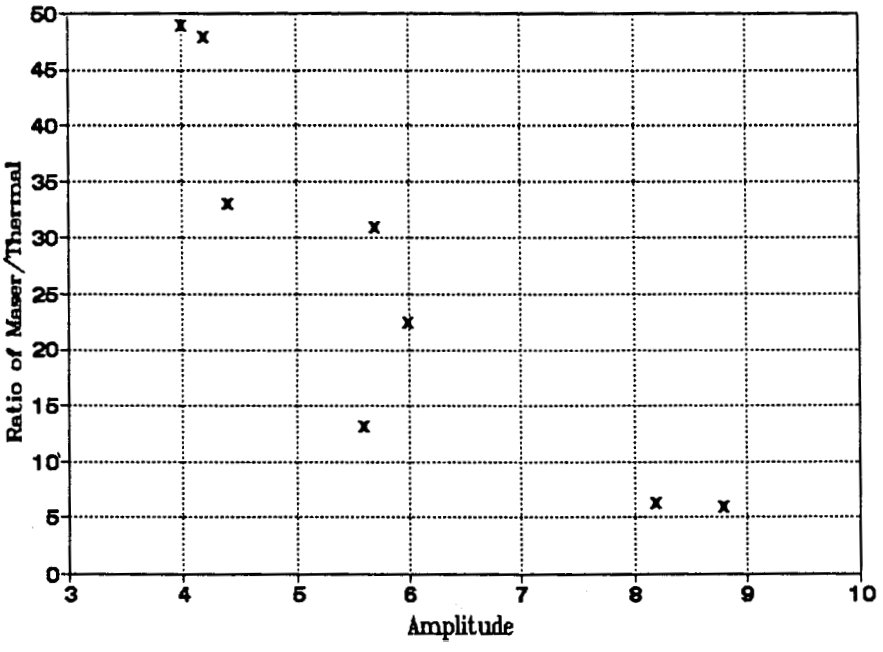

Figure 13: Anti-correlation between the ratio of SiO maser (v=1) to SiO thermal (v=0) flux and the visual amplitude of pulsation

are from Bujarrabal (1986). We find no correlation between the thermal emission and the visual amplitude of pulsation. Fig. 13 shows an indication of an anti-correlation between the strength of the maser and the amplitude of pulsation. The visual pulsational amplitude may have severe molecular blanketing effects (Lockwood and Wing 1971, Whitelock 1990), thus, as a more reliable representative of the changes in radius and temperature of the star, one should use the pulsational amplitude at infra-red wavelengths at which one can ignore the molecular absorptions in the atmosphere of the Mira variable. We have replotted Fig. 13 with this consideration, as Fig. 14, which now shows the ratio of the SiO maser flux to SiO thermal flux as a function of the amplitude of pulsation at 1.04 microns. The tentative trend of larger maser luminosity for lower pulsational amplitude is seen to remain in this plot but the correlation does not seem to be a strong one.

It is important to note that the correlations we have discussed are independent of each other. The bolometric-magnitudes, spectral-types and amplitudes of pulsation for stars in our sample, do not show any correlation with each other as seen in Fig. 15.

We attempt to interpret these results in Chapter 7.

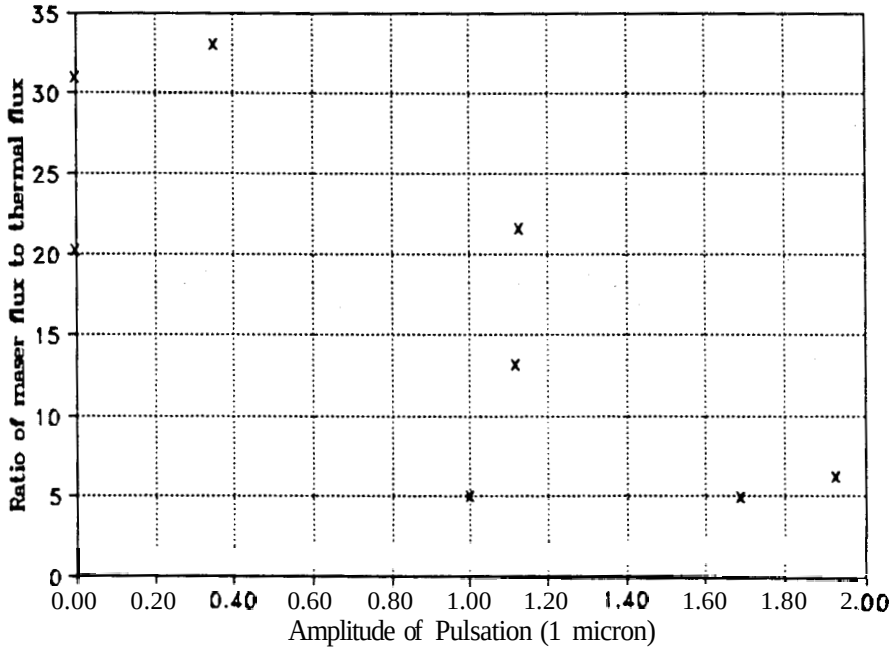

Figure 14: Same as Fig. 13, for pulsational amplitude at the wavelength of 1.04μ

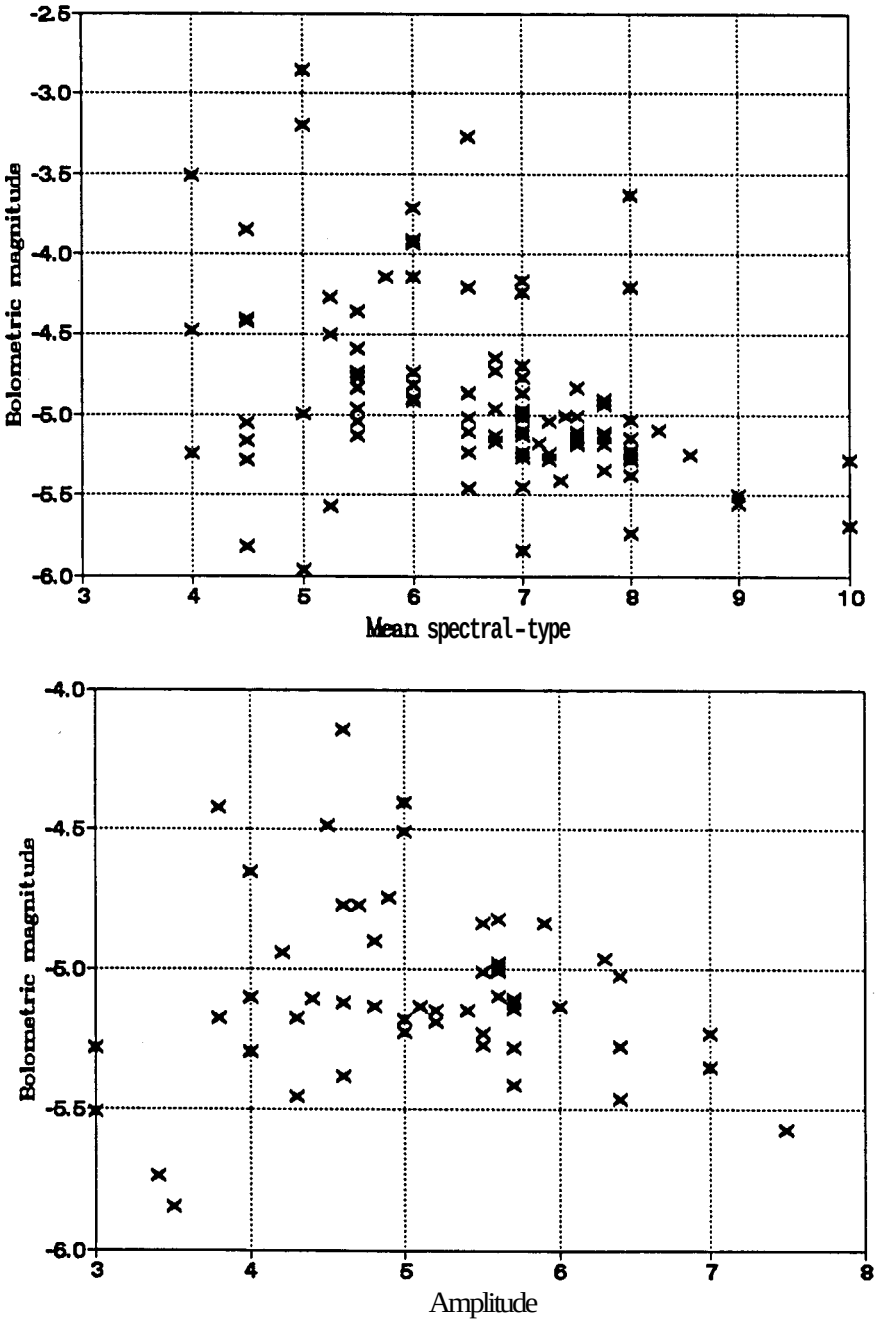

Figure 15: There is no correlation between the bolometric magnitudes, spectral-types, and the amplitudes of pulsation for stars in our sample

REFERENCES

Bessell M. S. et al., 1989, *Astron. Astrophys.* 213,209.

Bonneau *D.*, et al., 1982, *Astron. Astrophys* 106,235.

Bujarrabal V., et al., 1986, *Astron. Astrophys.* 162,157.

Cahn J.H., 1977, *Ap. J.* **212**,L135.

Dickinson D. F. et al., 1978, *Astron.* **J. 83**,36.

Dyck H. M., Lockwood G. W., Capps R. W., 1974, *Ap.* **J., 189**,89.

Kholopov P. N. et al. (Ed.), 1985, General Catalogue of Variable Stars, (Moscow Publishing House).

Keenan P. C., Garrison R. F., Deutsch **A. J.**, 1974, Ap. J. *Suppl. Ser.* 28,271.

Labeyrie A.. et al., 1977, *Ap.* **J.** *Lett.* **218**,L75.

Lockwood *G.* R., Wing R. F., 1971, *Ap.* **J. 169**,63.

Pettit E., Nicholson S. B., 1933, *Ap.* **J.** 78,320.

Robertson B. S. C., Feast M. W., 1981 Mon. Not. Royal Astron. Soc. **196**,11i.

Spencer J. H., et al. 1977, *Astron. J.* 82,706.

Whitelock P. A., 1986, Mon. Not. Royal Astron. Soc. 219,525.

Whitelock P. **A.**, 1990, Anglo-Australian Observatory preprint 1990.

Scalo J. M., 1976, *Ap.* **J.** 206,474.

Tsuji T., 1981, *Astron. Astrophys.* **99**,48.

Wood P. R. et al., 1983, *Ap.* **J. 273**,66.